Astrophysics and Space Science
DOI 10.1007/sXXXXX-XXX-XXXX-X

Doppler Boosting, Superluminal Motion, and the Kinematics of AGN Jets

K. I. Kellermann • Y. Y. Kovalev • M. L. Lister • D. C. Homan • M. Kadler • M. H. Cohen • E. Ros, J. A. Zensus • R. C. Vermeulen • M. F. Aller and H. D. Aller

Abstract We discuss results from a decade long program to study the fine-scale structure and the kinematics of relativistic AGN jets with the aim of better understanding the acceleration and collimation of the relativistic plasma forming AGN jets. From the observed distribution of brightness temperature, apparent velocity, flux density, time variability, and apparent luminosity, the intrinsic properties of the jets including Lorentz factor, luminosity, orientation, and brightness temperature are discussed. Special attention is given to the jet in M87, which has been studied over a wide range of wavelengths and which, due to its proximity, is observed with excellent spatial resolution.

Most radio jets appear quite linear, but we also observe curved non-linear jets and non-radial motions. Sometimes, different features in a given jet appear to follow the same curved path but there is evidence for ballistic trajectories as well. The data are best fit with a distribution of Lorentz factors extending up to $\gamma \sim 30$ and intrinsic luminosity up to $\sim 10^{26}\,\mathrm{W\,Hz^{-1}}$. In general, gamma-ray quasars may have somewhat larger Lorentz factors than non gamma-ray quasars. Initially the observed brightness temperature near the base of the jet extend up to $\sim 5 \times 10^{13}$ K which is well in excess of the inverse Compton limit and corresponds to a large excess of particle energy over magnetic energy. However, more typically, the observed brightness temperatures are $\sim 2 \times 10^{11}$ K, i.e., closer to equipartition.

Keywords galaxies: active — galaxies: jets — galaxies: individual (M87) — quasars: general — radio continuum: galaxies — acceleration of particles

K. I. Kellermann

National Radio Astronomy Observatory, 520 Edgemont Road, Charlottesville, VA 22903–2475, U.S.A.

Y. Y. Kovalev

Max-Planck-Institut für Radioastronomie, Auf dem Hügel 69, 53121 Bonn, Germany, and Astro Space Center of Lebedev Physical Institute, Profsoyuznaya 84/32, 117997 Moscow, Russia

M. L. Lister

Department of Physics, Purdue University, 525 Northwestern Avenue, West Lafayette, IN 47907, U.S.A.

D. C. Homan

Department of Physics and Astronomy, Denison University, Granville, OH 43023, U.S.A.

M. Kadler

Astrophysics Science Division, NASA Goddard Space Flight Center, Greenbelt Road, Greenbelt, MD 20771, U.S.A.

M. H. Cohen

Department of Astronomy, Mail Stop 105-24, California Institute of Technology, Pasadena, CA 91125, U.S.A.

E. Ros, J. A. Zensus

Max-Planck-Institut für Radioastronomie, Auf dem Hügel 69, 53121 Bonn, Germany

R. C. Vermeulen

Netherlands Foundation for Research in Astronomy, Postbus 2, NL-7990 AA Dwingeloo, Netherlands

M. F. Aller and H. D. Aller

Department of Astronomy, University of Michigan, 817 Denison Building, Ann Arbor, MI 48109–1042, U.S.A.

1 Introduction

More than 40 years ago, Shklovsky (1964) argued that the optical jet in M87 and in quasars such as 3C 273 appeared anisotropic due to differential Doppler boosting. Shklovsky realized that since radio galaxies such as Cygnus A typically have symmetric lobes, the jets which feed the radio lobes must also be two sided, but that they appear one sided due to differential relativistic Doppler beaming.

For the past decade, we have been using the NRAO Very Long Baseline Array (VLBA) at 2 cm wavelength to study the relativistic flow in AGN jets (Kellermann *et al.* 1998, 2004; Zensus *et al.* 2002; Kovalev *et al.*

2005; Lister 2005; Lister and Homan 2005). These observations have a nominal resolution of about 1 milliarcsec (mas) and are complemented by multi-epoch spectral observations at the RATAN-600 (Kovalev *et al.* 1999, 2002) and University of Michigan radio telescopes (Aller *et al.* 1985; Aller, Aller, and Hughes 2003) to determine "light-curves" over a wide range of frequencies. Our 2 cm VLBA observations are also complemented by observations made by Vermeulen *et al.* (2003) who have used the VLBA at 6 cm to study motions in nearly 300 sources from the Caltech-Jodrell Flat Spectrum sample. Jorstad *et al.* (2001, 2005) have observed a smaller number of sources at multiple epochs with the VLBA at 7mm wavelength with even higher angular resolution, while Piner *et al.* (2007) have used the VLBA along with a global array to study jet kinematics at 3.5 cm.

It is widely believed that the central engine which powers these radio and optical jets is due to accretion onto a super-massive black hole. We want to know where and how the jet plasma flow gets collimated and accelerated to relativistic velocities and whether or not there are accelerations or decelerations along the jet. We also want to know the intrinsic Lorentz factor, $\gamma = (1-\beta^2)^{-1/2}$, the intrinsic luminosity, L_o, and the intrinsic brightness temperature, T_o, where β is the speed of the relativistic plasma normalized to the speed of light. What determines these intrinsic jet properties and are they are related to other observables such as the variability or luminosity at other wavelengths?

1.1 Basic Relations

All quantitative values given in this paper are based on a cosmology with $H_0 = 70$ km s^{-1} Mpc^{-1}, $\Omega_{\rm m} = 0.3$, and $\Omega_\Lambda = 0.7$.

Due to relativistic effects, we observe apparent jet speeds, luminosities, and brightness temperatures which are related to the corresponding intrinsic quantities in the AGN rest frame through the Doppler factor, δ, the Lorentz factor, γ, and the jet orientation, θ, with respect to the line of sight.

The apparent velocity, $\beta_{\rm app}$, the apparent luminosity, L, the apparent brightness temperature, $T_{\rm app}$ and the Doppler factor, δ, can be calculated from the Lorentz factor, γ, the angle θ to the line of sight, and the intrinsic luminosity, L_o.

The apparent velocity $\beta_{\rm app}$ is given by

$$\beta_{\rm app} = \frac{\beta \sin\theta}{1-\beta\cos\theta}\,, \tag{1}$$

and the apparent luminosity, L, by

$$L = L_o \delta^n\,, \tag{2}$$

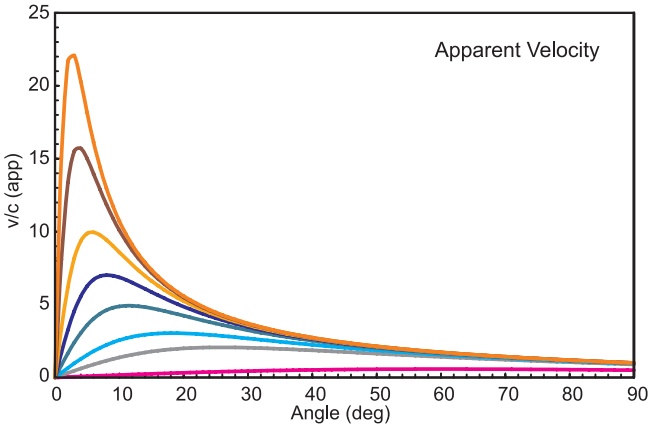

Fig. 1.— Apparent velocity vs. orientation for various values of intrinsic velocity. Red: $\beta = 0.5$, $\gamma = 1.15$; grey: $\beta = 0.9$, $\gamma = 2.3$; light blue: $\beta = 0.95$, $\gamma = 3.2$; green: $\beta = 0.98$, $\gamma = 5.0$; purple: $\beta = 0.99$, $\gamma = 7.1$; yellow: $\beta = 0.995$, $\gamma = 10.0$; brown: $\beta = 0.998$, $\gamma = 15.8$; orange: $\beta = 0.999$, $\gamma = 22.4$.

where the Doppler factor, δ, is

$$\delta = \gamma^{-1}(1-\beta\cos\theta)^{-1}\,, \tag{3}$$

and where L_o is the luminosity that would be measured by an observer in the AGN frame, and n depends on the geometry and spectral index and is typically in the range between 2 and 3. The apparent brightness temperature, $T_{\rm obs}$ is given by

$$T_{\rm obs} = \delta T_{\rm int}\,, \tag{4}$$

and the Lorentz factor, γ by

$$\gamma = (1-\beta^2)^{-1/2}. \tag{5}$$

In Figure 1, we show a plot of the apparent velocity, $\beta_{\rm app}$, versus orientation angle for various values of intrinsic speed, β. The maximum velocity is equal to γ and occurs at an angle $\theta_{\rm c} = \gamma^{-1}$. When $\theta = \theta_{\rm c}$, $\delta \sim \beta_{\rm app}$. Figure 2 shows the effect of Doppler boosting which reaches a factor of $\sim 10^4$ for $\gamma = 10$ ($\beta = 0.995$) and $n = 3$.

Assuming that the observed jet speeds, which are due to pattern motion, reflect the bulk jet flow velocity which is responsible for luminosity beaming, equations 1 to 5 may be used to derive the intrinsic values of γ, δ and $T_{\rm b}$.

Due to inverse Compton cooling, the maximum sustained peak intrinsic brightness temperature, $T_{\rm int}$, is less than about $10^{11.5}$ K. Close to this value, the energy in relativistic particles greatly exceeds the energy in magnetic fields (Kellermann and Pauliny-Toth 1969). If

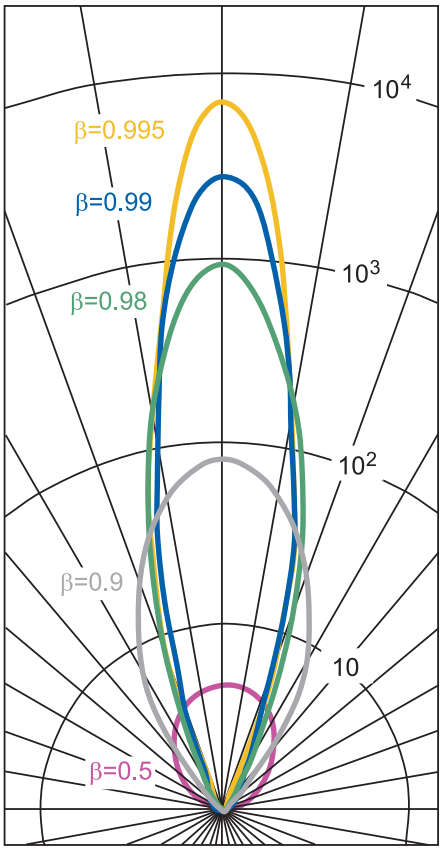

Fig. 2.— Luminosity Doppler boosting factor for the case where n=3 shown in polar coordinates. The radial lines indicate angles at intervals of 10 degrees and the circles the luminosity boosting factor. Red: $\beta = 0.5$, $\gamma = 1.15$; grey: $\beta = 0.9$, $\gamma = 2.3$; green: $\beta = 0.95$, $\gamma = 3.2$; blue: $\beta = 0.98$, $\gamma = 5.0$; $\beta = 0.99$, $\gamma = 7.1$; $\beta = 0.995$, $\gamma = 10.0$.

on the other hand the source is near equilibrium where the particle energy is close to the magnetic energy, then, $T_{\rm int} \sim 10^{10.5}$ K (Readhead 1994).

2 Radio jet structure

As a result of Doppler boosting, most AGN jets such as seen in PKS 1148−001 (Figure 3) appear asymmetric. However some jets with small Doppler factors, especially those associated with galaxies such as NGC 1052 (Figure 4) appear more symmetric.

Most of the jets we have observed are fairly straight, but some, such as the GPS radio galaxy PKS 1345+125 have pronounced curvature (see Figure 5 and Lister *et al.* 2003). In other sources, such as CTA 102 (Figure 6) and BL Lac (Denn, Mutel, and Marscher 2000), there is evidence of a helical structure.

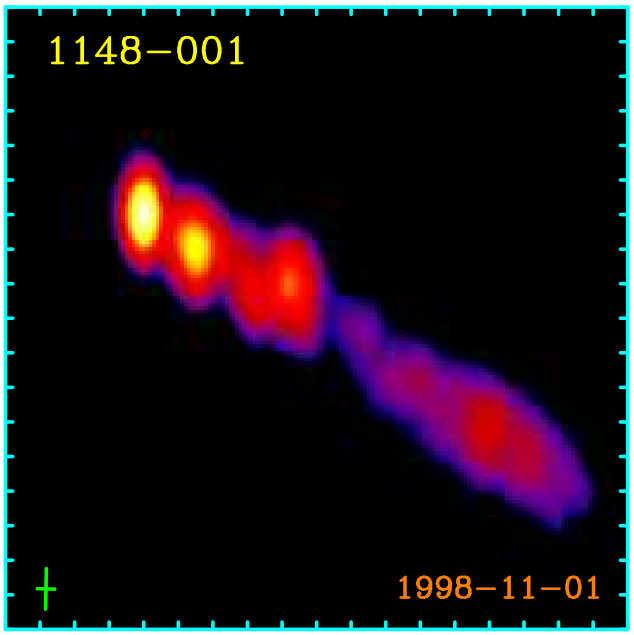

Fig. 3.— 2 cm VLBA image of the one sided jet in the quasar PKS 1148−001. The tick marks are spaced 1 mas apart.

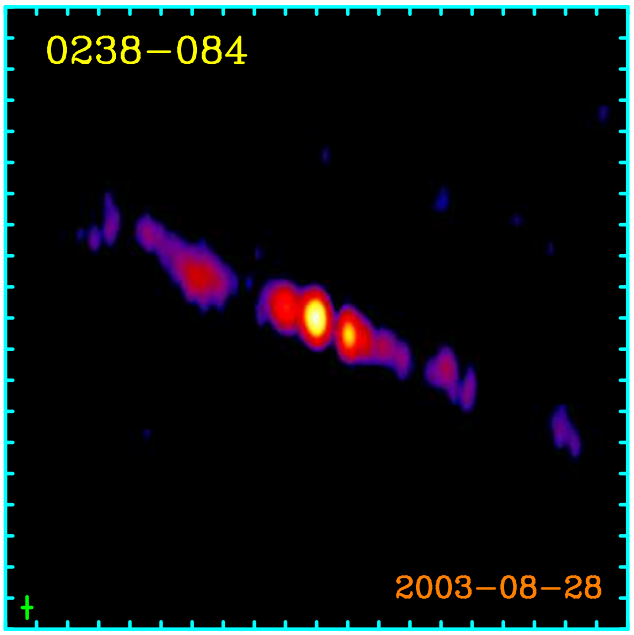

Fig. 4.— 2 cm VLBA image of the symmetric jets in the radio galaxy NGC 1052. The tick marks are spaced 2 mas apart.

In more than half of the sources, the base of the jet appears unresolved and is smaller than 0.05 mas in at least one dimension (Kovalev *et al.* 2005). This has interesting implications for jet physics. (See Section 3.2.)

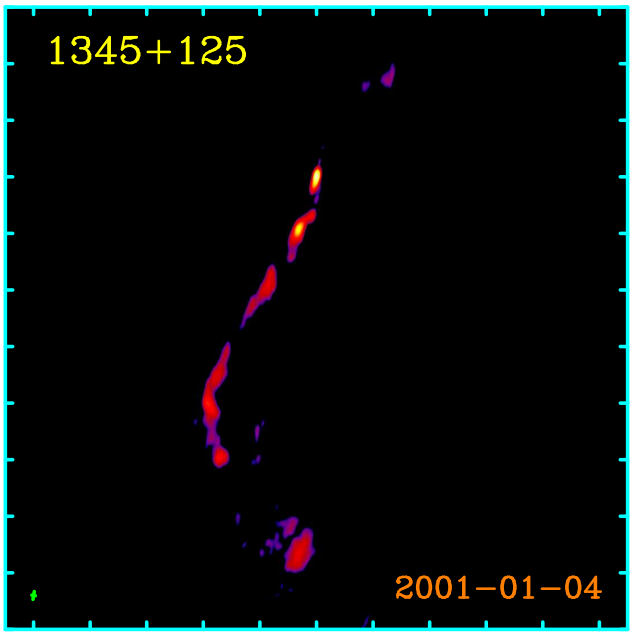

Fig. 5.— 2 cm VLBA image of the curved jet in the GPS radio galaxy PKS 1345+125. The tick marks are spaced 10 mas apart.

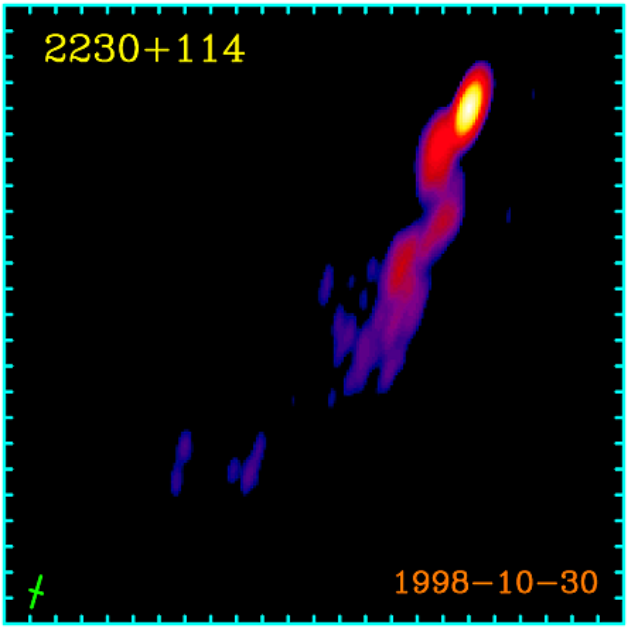

Fig. 6.— 2 cm VLBA image of CTA 102 showing a helical jet. The tick marks are spaced 2 mas apart.

Fig. 7.— HST image of the M87 jet.

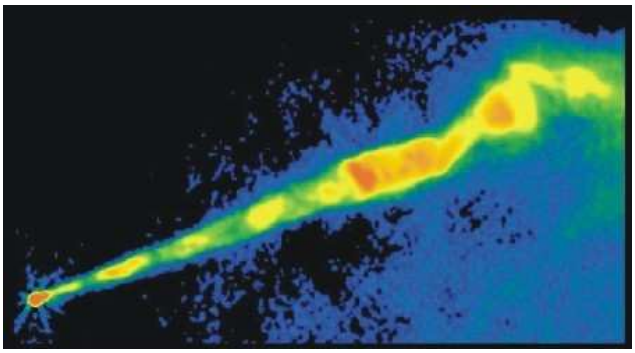

Fig. 8.— VLA 2 cm image of the M87 jet made with a resolution of 0.1 arcsec or 8 pc. Taken from Owen, Hardee, and Cornwell (1989).

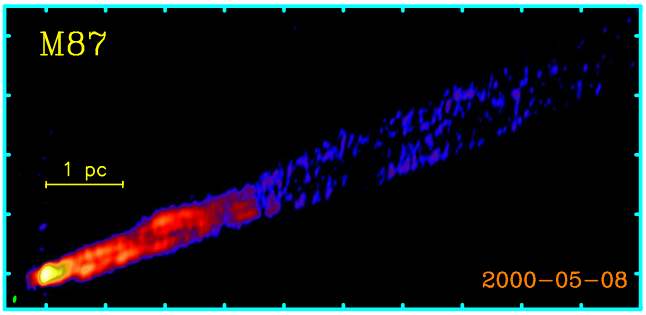

Fig. 9.— VLBA 2 cm image of the M87 jet. The tick marks are spaced 10 mas apart, and the resolution is about 1 mas = 0.08 parsec. This high dynamic range image which traces the jet out to nearly 0.1 arc sec was obtained from a full sky track using the VLBA along with one VLA antenna to increase the effective field of view. Adapted from Kovalev *et al.* (2007).

2.1 The radio galaxy M87

The radio source associated with M87 was one of the first to be recognized as being of extragalactic origin. It remains of great interest today, since at a distance of 16 Mpc, it is one of the closest radio galaxies. The VLBA linear scale of 1 mas = 0.08 pc is sufficient to resolve the M87 jet transverse to its extent and to study kinematics within a few tenths of a parsec from the central engine.

Figure 7 shows the HST optical image of the M87 jet, and Figure 8 the VLA 2 cm image, each with a resolution of about 0.1 arcsec. The morphology at radio, optical, and even X-ray wavelengths is very similar, suggesting a common synchrotron radiation mechanism at all wavelengths. At least at optical and X-ray

wavelengths, the electron lifetime down the jet is much shorter than the travel time from the nucleus, so there must be continual acceleration of relativistic particles within the jet itself (Harris and Krawczynski 2006).

In Figure 9, we show the 2 cm VLBA image with a resolution of about 1 mas (Kovalev *et al.* 2007). The VLBA image shows an apparent bifurcation of the inner jet, starting about 5 mas (0.4 pc) from the core. However, it is not clear if the apparent gap which extends along the center of the jet axis is due to an actual splitting of the jet, or if there is a thin cylindrical jet which appears limb brightened. The appearance of limb brightening may be the result of a spine-sheath configuration in which a faster inner jet is beamed in a more narrow cone away from the observer. The VLBA image also shows evidence of an apparent "counter-jet" extended toward the southeast.

Observations of the M87 jet made over more than a decade by Kovalev *et al.* (2007) indicate apparent jet flow speeds ranging from nearly stationary up to about $0.6c$. This is characteristic of radio galaxy jets such as observed in NGC 1052 (Vermeulen *et al.* 2003).

Considering that M87 was suggested by Shklovsky as the archetypical asymmetric Doppler boosted jet, its apparent velocity appears surprisingly "slow," although from equations 2 and 3, for orientations within about 30° from the line of sight, the jet to counter-jet ratio can be up to several orders of magnitude even for mildly relativistic velocities with $\gamma \sim 2$. It should also be noted that faster speeds have been observed further downstream (e.g., Biretta, Sparks, and Macchetto 1999).

3 Jet Kinematics

Repeated observations of quasar jets show values of $\beta_{\rm app}$ ranging up to about 30, corresponding to intrinsic velocities greater than 99.9 percent of the speed of light, while radio galaxy and BL Lac jets are typically much slower with subluminal apparent velocities. For example, in NGC 1052 we find only relatively slow jet motions with a velocity of 0.27c. We only see outward flows and do not see any motions with significant inward motion toward the jet base, although many features appear stationary. While there are significant differences in the apparent velocity of different jet features, the velocity spread from source to source is greater than within an individual jet. Kellermann *et al.* (2004) suggested that there is a characteristic speed for each jet which is probably reflected by the fastest observed jet feature.

In general, the observed motions can usually be described by a uniform velocity which is pointed radially outward from the base of the jet. Sufficiently long VLBA time baselines are now being obtained so that it is possible to detect in some individual cases non radial motions. In some jets the motion appears to follow the pre-existing path of earlier features (Kellermann *et al.* 2004). In other sources, the motion appears ballistic, but with different features moving in different directions, and there is some evidence for periodicities which may be the result of a precessing jet nozzle. Homan *et al.* (2003) have reported an abrupt change in the apparent trajectory of the nearly aligned jet in 3C 279 and have suggested that the final jet collimation is still occuring more than a kiloparsec downstream from the base.

In order to understand the jet physics, we want to be able to derive the intrinsic parameters from the observations of apparent speed, luminosity, and brightness temperature. We consider three approaches to estimate the Doppler factors along with the intrinsic Lorentz factor, rest frame luminosity, and rest frame brightness temperatures.

3.1 The $\beta_{\rm app}$ – luminosity relation

From equations 1 and 2 both the apparent velocity and apparent luminosity depend on the intrinsic speed and orientation. Thus, we might expect to see a relation between observed speed and observed luminosity. Cohen *et al.* (2007) have shown that the distribution of observed speed and luminosity is consistent with relativistic beaming models having a maximum value $\gamma_{\rm max} \approx 32$, and $L_{o,\rm max} \sim 10^{26}\,{\rm W\,Hz^{-1}}$. Figure 10 shows the distribution of observed values in the $\beta_{\rm app}$ – luminosity plane. There are no low luminosity sources with fast motions, but the high luminosity sources show a wide range of apparent speeds. The solid line represents the locus of points corresponding to $\gamma_{\rm max} \approx 32$, and $L_{o,\rm max} \sim 10^{26}\,{\rm W\,Hz^{-1}}$ which forms a close envelope to the data. The curve has a peak value near the critical angle $\theta_c = \gamma^{-1} \sim 3$ deg. Vermeulen and Cohen (1994) and Lister and Marscher (1997) have shown that the most probable angle to observe a source is when $\theta \sim 0.6\theta_c$ where $\beta_{\rm app} \sim 0.9\gamma$, so in any jet sample there will be some jets which are oriented close to $\theta_{\rm c}$ where $\beta_{\rm app} \approx \gamma$. Cohen *et al.* (2007) have concluded from the observed speed — luminosity distribution that $\gamma_{\rm max} \sim 32$ and that intrinsic luminosities may extend up to about $10^{26}\,{\rm W\,Hz^{-1}}$.

Cohen *et al.* (2007) have called attention to the galaxies and BL Lacs located in the lower left part of Figure 10. These sources are unlikely to be powerful

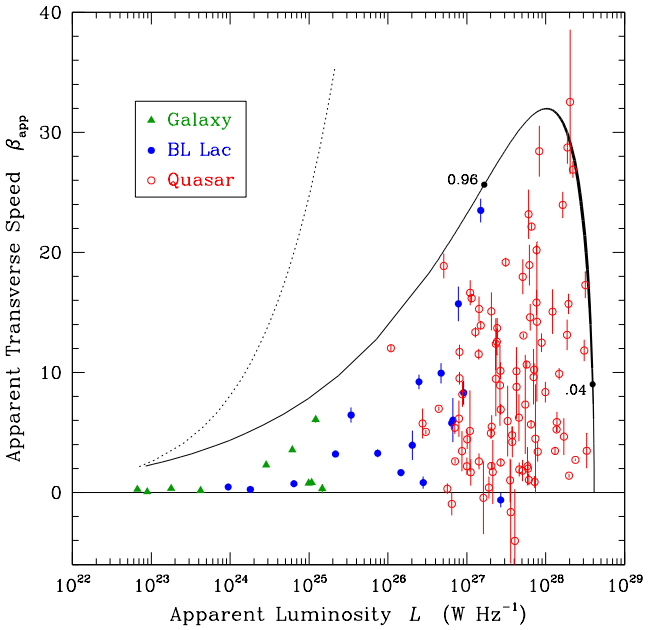

Fig. 10.— Plot of apparent transverse speed, $\beta_{\rm app}$, vs. apparent luminosity, L, for the fastest component in 119 well observed sources in the 2 cm VLBA surveys. The curve shows the locus of points, $(\beta_{\rm app}, L)$, for sources with $\gamma_{\rm max} \approx 32$, and $L_o \sim 10^{26}\,{\rm W\,Hz^{-1}}$. The viewing angle increases from zero going from right to left. The thickness of the line corresponds to the probability that a source will be observed at a given location on the curve, and the locations of the 4 and 96 percent probability points are labeled. The dotted line represents an observational limit determined by the weakest sources included, $S_{\rm VLBA,med} = 0.5\,{\rm Jy}$, and the fastest detectable angular motions of $\mu = 4\,{\rm mas\,yr^{-1}}$ set by our sampling interval of a few times per year. Red open circles represent quasars; blue full circles, BL Lacs; and green triangles, galaxies. Adopted from Cohen *et al.* (2007).

quasar jets oriented close to the plane of the sky as might be expected from simple unified models (Urry and Padovani 1995), nor can they be high – γ, low – L_o jets beamed very close to the line of sight as the probability of these configurations is too low. Instead, in general, the galaxies and BL Lacs must form a separate class of low luminosity jets. However, the powerful radio galaxy Cygnus A has only a relatively weak jet with $0.59 < \beta < 0.68$. Following the simulations of Agudo *et al.* (2001), Cohen *et al.* (2007) have suggested that the Cygnus A jet has a spine-sheath structure with an energetic fast spine beamed away from the line of sight to feed the powerful extended lobes and enshrouded by a slower observed sheath whose broader but weaker beam encompasses the line of sight.

3.2 The $\beta_{\rm app}$ – $T_{\rm b}$ relation

The brightness temperature of jet features may be determined directly from observations, or estimated from the time scale of flux density variations. Each of these methods gives separate insight to the physics of AGN jets. The measured peak brightness temperature is typically in the range 10^{11-13} K but extends up to 5×10^{13} K (Kovalev *et al.* 2005). Observations with longer baselines, such as will be possible with the planned Russian and Japanese space VLBI missions, will be needed to determine whether higher brightness features can exist.

Homan *et al.* (2006) have used the peak brightness temperature at the base of each jet observed by Kovalev *et al.* (2005) to study the dependence of apparent speed, $\beta_{\rm app}$, on apparent peak brightness temperature, $T_{\rm b}$. Figure 11 shows plots of $\beta_{\rm app}$ versus the maximum observed brightness (upper plot) temperature and versus a more typical "median-low" value of brightness temperature. In both cases, the solid line represents sources observed at the critical angle (γ^{-1}) corresponding to the value of intrinsic brightness temperature,$T_{\rm int}$, and the same value for $T_{\rm int}$ is used in calculating the dotted "envelope." These values of $T_{\rm int}$ were chosen so that approximately 75% of the sources would fall below and to the right of the solid line corresponding to what was found from simulations reported by Homan *et al.* (2006).

In both plots, the highest velocities are seen only for sources with high apparent brightness temperature, and there is a clear absence of fast sources with low brightness temperatures, as is also indicated by the simulations. Homan *et al.* (2006) have therefore concluded that there is a relatively narrow range of intrinsic brightness temperatures extending perhaps a factor of two on either side of the solid line shown in Figure 11. Since, the plot of maximum brightness temperature contains more lower limits than measurements, when in their high state, the brightness temperature must be more than 2×10^{11} K, which corresponds to a large excess of particle energy over magnetic energy (Kellermann and Pauliny-Toth 1969; Readhead 1994). However, in the median-low state, $T_{\rm int}$ is closer to the equilibrium value where the particle energy is about the same as the magnetic energy.

3.3 The $\beta_{\rm app}$ – $D_{\rm var}$ relation

Most compact radio sources are variable on time scales typically of months to years, (e.g., Kovalev *et al.* 2002; Aller, Aller, and Hughes 2006). An independent estimate of the Doppler factor can be obtained from the

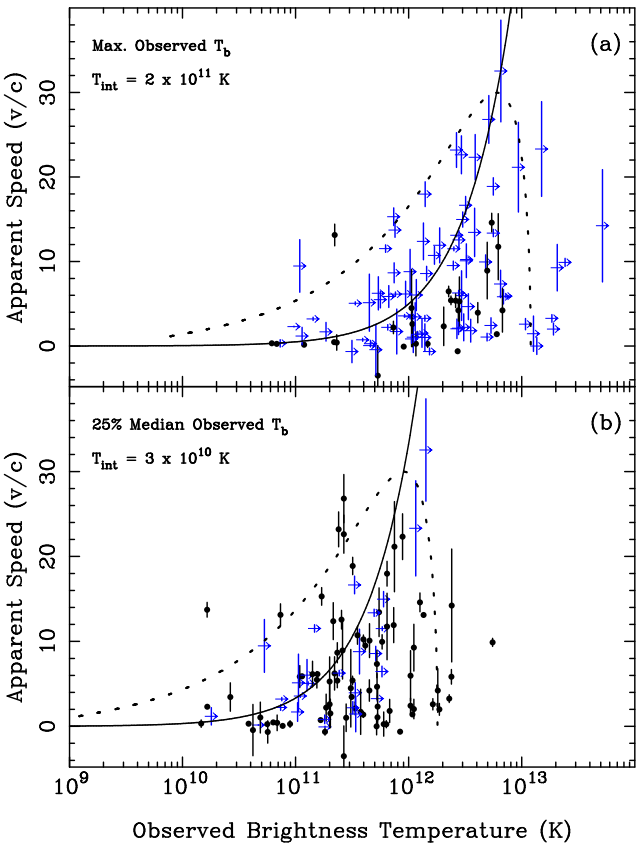

Fig. 11.— Plots of apparent speed, $\beta_{\rm app}$, vs. observed peak jet brightness temperature, $T_{\rm b}$. Lower limits are indicated in blue by arrows. The upper panel is based on the peak value of $T_{\rm b}$ observed for each source, while the lower panel contains a similar plot, except that it shows sources in their median-low state, what Homan *et al.* (2006) called the "25% Median." This 25% median is the median of the lowest half of the brightness temperature observations for a given source and represents a typical low brightness state for each source. The solid line shown in each plot represents sources observed at the critical angle that has the intrinsic brightness temperature indicated in the upper left hand corner of the panel. The dashed line represents the possible apparent speeds of a $\gamma = 30$ source with intrinsic brightness temperature given by the value of $T_{\rm int}$. Adapted from Homan *et al.* (2006).

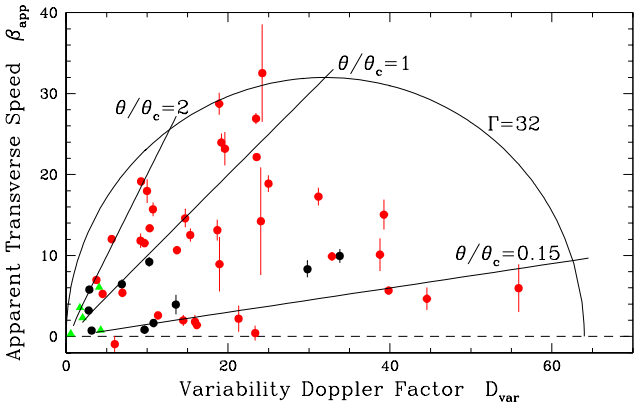

Fig. 12.— Plot of apparent transverse speed, $\beta_{\rm app}$, vs. $D_{\rm var}$ for components in 49 sources in the NRAO 2-cm VLBA survey. The Doppler factor, $D_{\rm var}$ is derived from the variability time scale near 1 cm, assuming an intrinsic brightness temperature of 2×10^{10} K. The semi circle represents the locus of points with a Lorentz factor, $\gamma = 32$ as θ varies from 0 to 360 degrees. The straight lines represent angles with respect to the line of sight in terms of the critical angle $\theta_{\rm c}$ where $\delta_{\rm var} = \beta_{\rm app}$. Red open circles are quasars; blue full circles, BL Lacs; and green triangles, galaxies. Adopted from Kellermann *et al.* (2004).

time scale of the observed variability. In the absence of any relativistic effects, the linear dimensions are limited to the light travel distance on the time scale of the variability. This puts a theoretical upper limit on the linear size and consequently an upper limit on the angular size and corresponding lower limit to the brightness temperature. However, due to relativistic boosting, the timescale for variability (and thus T_{var}) as well as for $\beta_{\rm app}$ are both compressed. The apparent brightness temperature in this case is given by

$$T_{var} = \delta^3 T_{\rm int} \, . \qquad (6)$$

Equation 6 differs from equation 4 in that the observed brightness temperature depends on δ^3 rather than δ. In equation 6 two powers of δ are due to the solid angle which is determined from the time variability. The third factor of δ follows from the beaming as given in equation 2.

Following Lähteenmäki and Valtaoja (1999), Kellermann *et al.* (2004) and Cohen *et al.* (2003) estimated the Doppler factor, $\delta_{\rm var}$, for 49 sources from the time scale of flux density variability measured near 1 cm. The plot for $T_{\rm int} = 2 \times 10^{10}$ K gives the best fit between our observed data and simulations based on a power law distribution of luminosity and γ. Figure 12 shows a modified version of $\beta_{\rm app}$, vs. $\delta_{\rm var}$ plot using updated values of $\beta_{\rm app}$ from the MOJAVE program. The best fit value of $T_{\rm int} = 2 \times 10^{10}$ K is in good agreement with the independently determined equilibrium value of $T_{\rm int}$ found from the distribution of peak values of $T_{\rm b}$ obtained from the direct VLBA measurements (Figure 11) and is significantly less than the inverse Compton limit of $\sim 5 \times 10^{11}$ K.

3.4 Finite opening angles

The quantitative discussion in this section assumes that the jet is one dimensional. Gopal-Krishna, Wiita, and Dhurde (2006) and Wiita *et al.* (2006) have discussed the implications of finite opening angles and a non uniform velocity across the jet cone. They also consider the special case where the viewer is inside the opening angle of the jet. They argue that if the jet opening angle is sufficiently large, then the Lorentz factors calculated under the assumption of a one dimensional jet may be substantially underestimated.

4 Radio Jets and Gamma-Ray Emission

Many gamma-ray bright sources are identified with flat spectrum radio AGN (Mattox, Hartman, and Reimer 2001; Harris *et al.* 2003; Sowards-Emmerd, Romani, and Michelson 2003). However, comparison of radio jet structure or kinematics with gamma-ray emission has been inconclusive. Kellermann *et al.* (1998) reported no difference in the morphology of AGN jets with and without observed gamma-ray emission, but Kovalev *et al.* (2005) found that the radio jets of gamma-ray sources appear to have more compact structure than non gamma-ray sources. Kellermann *et al.* (2004) and Jorstad *et al.* (2001) reported evidence that AGN with observed gamma-ray emission have somewhat higher observed speeds, but this was based on the very limited gamma-ray data obtained by the EGRET detector on the Gamma Ray Observatory. The start of GLAST operations in 2008 will give greatly improved sensitivity and time sampling for thousands of gamma-ray sources and will establish whether there is a substantial increase in the number of gamma-ray detections, or if instead, there is a class of "gamma-ray quiet" quasars analogous to radio-quiet quasars. Our planned extension of the MOJAVE program through the GLAST era will give us a better understanding of the relation between the radio jets and gamma-ray emission.

5 Summary

VLBA observations have led to an increased understanding of the nature of AGN jets including the following:

1. Trends of observed velocity with luminosity, brightness temperature, and variability are consistent with relativistic beaming models in which blazar jets are highly relativistic with Lorentz factors extending up to about 30 and are oriented close the line of sight.
2. There is a broad distribution of Lorentz factors among observed sources. The parent population contains jets which are mostly only mildly relativistic. However, due to Doppler boosting bias, in flux density limited samples we see mostly the ultra-relativistic jets. But, some of the slower jets are also directly observed.
3. The collimation and acceleration appear to occur close to the central engine, but *in situ* acceleration within the jet is also important, and the final collimation in some cases may be determined up to a kiloparsec or more downstream.
4. Each jet appears to have a characteristic velocity which may reflect the bulk plasma flow. In general, features observed at shorter wavelengths, which are closer to the core, appear to move with higher speed. Quasar jets typically have apparent speeds around $10c$, corresponding to intrinsic speeds of 99.9 percent of the speed of light. Apparent speeds up to about $35c$ are observed in some quasars. Lower luminosity AGN, the cores of extended FR I and FR II radio galaxies, and BL Lac objects usually appear much slower with apparent velocities which are close to the speed of light and may even appear subluminal.
5. Radio jets associated with gamma-ray sources appear to have, on average, more compact structure and show faster outflow speeds.
6. Initially, following the injection of new relativistic particles, intrinsic (in the source frame) brightness temperatures up to a few times $T_{\rm int} \sim 10^{11}$ K are inferred corresponding to an apparent excess of particle energy over the energy in magnetic fields. But the energy balance later approaches equilibrium corresponding to $T_{\rm int} \sim 5 \times 10^{10}$ K.
7. The overall kinematics of the jets are rather complex, with some jets displaying bright features moving on linear trajectories, while others have accelerated motions on curved trajectories. In many sources, successive features are ejected on different sky position angles, and do not follow the paths of previous knots.
8. The quantitative analysis and derivation of intrinsic properties may be complicated by possible differences between the pattern and bulk velocity flow as well as by the finite opening angle of jets and possible velocity or density gradients across the jet.

In the next few years, improved data recording systems will allow better sensitivity so that it will be possible to trace the structure further along the jets and to follow the motion of individual features for a longer time. The improved sensitivity will also permit more routine observations at shorter wavelengths with corresponding better angular resolution. The availability of the GLAST all-sky gamma-ray data with high sensi-

tivity and good time resolution should enhance our understanding of the connections between radio jets and gamma-ray emission.

6 Data Archive

All of our images, movies, the RATAN spectral monitoring from 1.4 to 30 cm, and all kinematic data are available on our web site[1]. Flux densities measured at the UMRAO at 2, 4, and 6 cm can be found at the UMRAO Database[2] and more up to date data may be obtained by contacting the UMRAO authors.

Since 2002, we have extended our observations to include measurements of circular and linear polarization (Lister and Homan 2005; Homan and Lister 2006). Polarization data are given on our web site. However, discussion of the polarization properties of AGN jets is beyond the scope of this paper.

Acknowledgements This paper is based on observations made with the Very Long Baseline Array which is a facility of the National Radio Astronomy Observatory which is operated by Associated Universities, Inc., under a cooperative agreement with the National Science Foundation. Part of this work was done by YYK, MLL and DCH during their Karl Jansky postdoctoral fellowship at the National Radio Astronomy Observatory. YYK is currently a Research Fellow of the Alexander von Humboldt Foundation. DCH was partially supported by an award from the Research Corporation. MK was supported in part through a stipend from the International Max Planck Research School for Radio Astronomy at the University of Bonn and, in part, by a NASA Postdoctoral Program Fellowship appointment at the Goddard Space Flight Center. The MOJAVE project is supported under National Science Foundation grant AST-0406923 and a grant from the Purdue Research Foundation. The work at the RATAN-600 radio telescope was supported by the Russian Ministry of Education and Science, the NASA JURRISS Program (project W-19611), and the Russian Foundation for Basic Research (grants 01-02-16812 and 05-02-17377). The University of Michigan Radio Astronomy Observatory is supported by the University of Michigan and the National Science Foundation (grant AST-0607523).

References

Agudo, I., Gómez, J.L., Martí, J.M., Ibáñez, J.M., Marscher, A.P., Alberdi, A., Aloy, M.A., Hardee, P.E.: Jet Stability and the Generation of Superluminal and Stationary Components. ApJ 549, L183–L186 (2001). doi:10.1086/319158

Aller, H.D., Aller, M.F., Latimer, G.E., Hodge, P.E.: Spectra and linear polarizations of extragalactic variable sources at centimeter wavelengths. ApJS 59, 513–768 (1985). doi:10.1086/191083

Aller, M.F., Aller, H.D., Hughes, P.A.: Survey of Variability. In: Zensus, J.A., Cohen, M.H., Ros, E. (eds.) ASP Conf. Ser. 300: Radio Astronomy at the Fringe. pp. 159–168. (2003)

Aller, M.F., Aller, H.D., Hughes, P.A.: Radio-Band Observations of Blazar Variability. In: Miller, H.R., Marshall, K., Webb, J.R., Aller, M.F. (eds.) ASP Conf. Ser. 350: Blazar Variability Workshop II: Entering the GLAST Era. pp. 25–32. (July 2006)

Biretta, J.A., Sparks, W.B., Macchetto, F.: Hubble Space Telescope Observations of Superluminal Motion in the M87 Jet. ApJ 520, 621–626 (1999). doi:10.1086/307499

Cohen, M.H., Russo, M.A., Homan, D.C., Kellermann, K.I., Lister, M.L., Vermeulen, R.C., Ros, E., Zensus, J.A.: Variability and Velocity of Superluminal Sources. In: Zensus, J.A., Cohen, M.H., Ros, E. (eds.) ASP Conf. Ser. 300: Radio Astronomy at the Fringe. pp. 177–184. (2003)

Cohen, M.H., Lister, M.L., Homan, D.C., Kadler, M., Kellermann, K.I., Kovalev, Y.Y., Vermeulen, R.C.: Relativistic Beaming and the Intrinsic Properties of Extragalactic Radio Jets. ApJ 658, 232–244 (2007). doi:10.1086/511063

Denn, G.R., Mutel, R.L., Marscher, A.P.: Very Long Baseline Polarimetry of BL Lacertae. ApJS 129, 61–92 (2000). doi:10.1086/313403

Gopal-Krishna, , Wiita, P.J., Dhurde, S.: Bulk motion of ultrarelativistic conical blazar jets. MNRAS 369, 1287–1292 (2006). doi:10.1111/j.1365-2966.2006.10376.x

Harris, D.E., Krawczynski, H.: X-Ray Emission from Extragalactic Jets. ARA&A 44, 463–506 (2006). doi:10.1146/annurev.astro.44.051905.092446

Harris, D.E., Biretta, J.A., Junor, W., Perlman, E.S., Sparks, W.B., Wilson, A.S.: Flaring X-Ray Emission from HST-1, a Knot in the M87 Jet. ApJ 586, L41–L44 (2003). doi:10.1086/374773

Homan, D.C., Lister, M.L.: MOJAVE: Monitoring of Jets in Active Galactic Nuclei with VLBA Experiments. II. First-Epoch 15 GHz Circular Polarization Results. AJ 131, 1262–1279 (2006). doi:10.1086/500256

Homan, D.C., Lister, M.L., Kellermann, K.I., Cohen, M.H., Ros, E., Zensus, J.A., Kadler, M., Vermeulen, R.C.: Jet Collimation in Action: Realignment on Kiloparsec Scales in 3C 279. ApJ 589, L9–L12 (2003). doi:10.1086/375726

Homan, D.C., Kovalev, Y.Y., Lister, M.L., Ros, E., Kellermann, K.I., Cohen, M.H., Vermeulen, R.C., Zensus, J.A., Kadler, M.: Intrinsic Brightness Temperatures of AGN Jets. ApJ 642, L115–L118 (2006). doi:10.1086/504715

[1] http://www.physics.purdue.edu/astro/MOJAVE/

[2] http://www.astro.lsa.umich.edu/obs/radiotel/umrao.html

Jorstad, S.G., Marscher, A.P., Mattox, J.R., Wehrle, A.E., Bloom, S.D., Yurchenko, A.V.: Multiepoch Very Long Baseline Array Observations of EGRET-detected Quasars and BL Lacertae Objects: Superluminal Motion of Gamma-Ray Bright Blazars. ApJS 134, 181–240 (2001). doi:10.1086/320858

Jorstad, S.G., Marscher, A.P., Lister, M.L., Stirling, A.M., Cawthorne, T.V., Gear, W.K., Gómez, J.L., Stevens, J.A., Smith, P.S., Forster, J.R., Robson, E.I.: Polarimetric Observations of 15 Active Galactic Nuclei at High Frequencies: Jet Kinematics from Bimonthly Monitoring with the Very Long Baseline Array. AJ 130, 1418–1465 (2005). doi:10.1086/444593

Kellermann, K.I., Pauliny-Toth, I.I.K.: The Spectra of Opaque Radio Sources. ApJ 155, L71–L78 (1969)

Kellermann, K.I., Vermeulen, R.C., Zensus, J.A., Cohen, M.H.: Sub-Milliarcsecond Imaging of Quasars and Active Galactic Nuclei. AJ 115, 1295–1318 (1998). doi:10.1086/300308

Kellermann, K.I., Lister, M.L., Homan, D.C., Vermeulen, R.C., Cohen, M.H., Ros, E., Kadler, M., Zensus, J.A., Kovalev, Y.Y.: Sub-Milliarcsecond Imaging of Quasars and Active Galactic Nuclei. III. Kinematics of Parsec-scale Radio Jets. ApJ 609, 539–563 (2004). doi:10.1086/421289

Kovalev, Y.Y., Nizhelsky, N.A., Kovalev, Y.A., Berlin, A.B., Zhekanis, G.V., Mingaliev, M.G., Bogdantsov, A.V.: Survey of instantaneous 1-22 GHz spectra of 550 compact extragalactic objects with declinations from -30° to $+43^\circ$. A&AS 139, 545–554 (1999). doi:10.1051/aas:1999406

Kovalev, Y.Y., Kovalev, Y.A., Nizhelsky, N.A., Bogdantsov, A.B.: Broad-band Radio Spectra Variability of 550 AGN in 1997-2001. Publications of the Astronomical Society of Australia 19, 83–87 (2002). doi:10.1071/AS01109

Kovalev, Y.Y., Kellermann, K.I., Lister, M.L., Homan, D.C., Vermeulen, R.C., Cohen, M.H., Ros, E., Kadler, M., Lobanov, A.P., Zensus, J.A., Kardashev, N.S., Gurvits, L.I., Aller, M.F., Aller, H.D.: Sub-Milliarcsecond Imaging of Quasars and Active Galactic Nuclei. IV. Fine-Scale Structure. AJ 130, 2473–2505 (2005). doi:10.1086/497430

Kovalev Y.Y., Lister M.L., Homan D.C., Kellermann K.I.: The Inner Jet of the Radio Galaxy M87. ArXiv e-prints 0708.2695 (2007); ApJL, in press

Lähteenmäki, A., Valtaoja, E.: Total Flux Density Variations in Extragalactic Radio Sources. III. Doppler Boosting Factors, Lorentz Factors, and Viewing Angles for Active Galactic Nuclei. ApJ 521, 493–501 (1999). doi:10.1086/307587

Lister, M.L.: The MOJAVE Program: Studying the Relativistic Kinematics of AGN Jets. In: Romney, J., Reid, M. (eds.) ASP Conf. Ser. 340: Future Directions in High Resolution Astronomy. pp. 20–24. (December 2005)

Lister, M.L., Homan, D.C.: MOJAVE: Monitoring of Jets in Active Galactic Nuclei with VLBA Experiments. I. First-Epoch 15 GHz Linear Polarization Images. AJ 130, 1389–1417 (2005). doi:10.1086/432969

Lister, M.L., Marscher, A.P.: Statistical Effects of Doppler Beaming and Malmquist Bias on Flux-limited Samples of Compact Radio Sources. ApJ 476, 572–588 (1997). doi:10.1086/303629

Lister, M.L., Kellermann, K.I., Vermeulen, R.C., Cohen, M.H., Zensus, J.A., Ros, E.: 4C +12.50: A Superluminal Precessing Jet in the Recent Merger System IRAS 13451+1232. ApJ 584, 135–146 (2003). doi:10.1086/345666

Mattox, J.R., Hartman, R.C., Reimer, O.: A Quantitative Evaluation of Potential Radio Identifications for 3EG EGRET Sources. ApJS 135, 155–175 (2001). doi:10.1086/321782

Owen, F.N., Hardee, P.E., Cornwell, T.J.: High-resolution, high dynamic range VLA images of the M87 jet at 2 centimeters. ApJ 340, 698–707 (1989). doi:10.1086/167430

Piner, B.G., Mahmud, M., Fey, A.L., Gospodinova, K.: Relativistic Jets in the Radio Reference Frame Image Database. I. Apparent Speeds from the First 5 Years of Data. AJ 133, 2357–2388 (2007). doi:10.1086/514812

Readhead, A.C.S.: Equipartition brightness temperature and the inverse Compton catastrophe. ApJ 426, 51–59 (1994). doi:10.1086/174038

Shklovsky, I.S.: Nature of Jets in Radio Galaxies. Soviet Astronomy 7, 748–754 (1964)

Sowards-Emmerd, D., Romani, R.W., Michelson, P.F.: The Gamma-Ray Blazar Content of the Northern Sky. ApJ 590, 109–122 (2003). doi:10.1086/374981

Urry, C.M., Padovani, P.: Unified Schemes for Radio-Loud Active Galactic Nuclei. PASP 107, 803 (1995)

Vermeulen, R.C., Cohen, M.H.: Superluminal motion statistics and cosmology. ApJ 430, 467–494 (1994). doi:10.1086/174424

Vermeulen, R.C., Britzen, S., Taylor, G.B., Pearson, T.J., Readhead, A.C.S., Wilkinson, P.N., Browne, I.W.A.: Motion Statistics in the CJ Survey - The Status in October 2002. In: Zensus, J.A., Cohen, M.H., Ros, E. (eds.) ASP Conf. Ser. 300: Radio Astronomy at the Fringe. pp. 43–48 (2003)

Vermeulen, R.C., Ros, E., Kellermann, K.I., Cohen, M.H., Zensus, J.A., van Langevelde, H.J.: The shroud around the twin radio jets in NGC 1052. A&A 401, 113–127 (2003). doi:10.1051/0004-6361:20021752

Wiita, P.J., Gopal-Krishna, , Dhurde, S., Sircar, P.: Effects of Jet Opening Angle and Velocity Structure on Blazar Parameters. In: American Astronomical Society Meeting Abstracts. p. 08.09. (December 2006)

Zensus, J.A., Ros, E., Kellermann, K.I., Cohen, M.H., Vermeulen, R.C., Kadler, M.: Sub-milliarcsecond Imaging of Quasars and Active Galactic Nuclei. II. Additional Sources. AJ 124, 662–674 (2002). doi:10.1086/341585

This 2-column preprint was prepared with the AAS LaTeX macros v5.2.